A Facile Synthesis, Structural Elucidation and Biological Evaluation of dihydropyrimidinone compound

S. Shanmugam[1], K. Neelakandan[2], M. Gopalakrishnan[3] and S. Pazhamalai[4]

[1,3,4]Department of Chemistry, Annamalai University, Annamalainagar- 608 002, Tamilnadu, India

[2]Emcure Pharmaceuticals Limited, Pune–411 057, Maharashtra, India

[4]Corresponding author: *E-mail:* sripazhamalai@gmail.com Tel.: +91 9047982112

Abstract - *The chemical structure of the newly synthesized compound Ethyl-6-methyl-2-oxo-4-(3,4,5-trichlorophenyl)-1,2,3,4-tetrahydropyrimidine-5-carboxylate* **4** *was confirmed by elemental analysis, ^{1}H NMR, ^{13}C NMR, and ESI-HRMS spectral data. In addition, in the form of the complete and partial density of states, the HOMO-LUMO energy gap, and electrostatic potential map, etc., some quantum chemical insights have been obtained. Furthermore, to demonstrate the possible applications of dihydropyrimidinone* **4** *in nonlinear optics, the polarizability and first hyperpolarizability were measured. Molecular docking is also determined in order to illustrate the over expression of estrogen receptor in 92 % of 2J9M protein. The antitumor activity of these compound was evaluated on breast cancer (MCF-7) cell lines by a cell viability assay utilizing the tetrazolium dye 3-(4,5-dimethylthiazol-2-yl)-2,5-diphenyltetrazolium bromide (MTT). Although with varying degrees, a significant growth inhibitory and cytotoxic effect was observed on MCF-7 cancer cell line. The tested compound* **4**, *was active against MCF-7 cell line (in-vitro analysis) with IC_{50} values of 45 μM. The compound was subjected for the DPPH & ABTS tests, evaluated its antioxidant activity. With further characterization, mechanism of biological action, this compound 4 shall be a potential / useful candidate as anticancer drug.*

Keywords: *Synthesis; Dihydropyrimidinone; molecular docking; anticancer activity; antioxidant and DFT.*

1. INTRODUCTION

Noncommunicable diseases are a major threat to global health, causing a significant amount of death every year. Cancer is becoming a global burden, next to cardiovascular disease, which leads to the deaths of about 8.7 million in the year 2015 [1]. In addition, cancer is expected to rate as the prominent cause of death and is the most significant barrier for the increase of life expectancy in the world [2]. Further, cancer is a major health challenge not only in high-income countries but also in low and middle-income countries (LMICs), where the number of cancer patient is rapidly growing [3]. Since the majority of anticancer drugs are associated with serious side effects, scouting for novel chemical agents that are cytotoxic to cancer cells with less side effects are an utmost requirement. 3,4-Dihydropyrimidin-2(1*H*)-one (DHPM) is an important class of heterocyclic compound due to their various pharmacological properties. Since the first-time synthesis of dihydropyrimidinone over 100 years ago, a wide range of biological properties had been screened for them. Now a days DHPM derivatives have secured immense attraction for their various pharmacological properties and as such several drug candidates had been developed based on dihydropyrimidinone core.[5-12] Recently Singh

et al. were also able to study the effect of N-alkylated dihydropyrimidinone over swine carotid arteries in relaxing a membrane depolarization induced contraction of vascular smooth muscle.[13] The α1A-selective adrenoreceptor antagonist L-771,688 [14] effective against benign prostatic hyperplasia, also contains DMPM core structure. The mitotic kinesin Eg5 inhibitor Monastrol having excellent anti-cancer property [15-19] and a non-nucleosidic inhibitor of hepatitis B virus replication Bay 41-4109 [20] also possess DHPM moiety. It has been described that Biginelli compounds, dihydropyrimidinone are known to exhibit various interesting biological properties including antiviral [21,22], antitumor [23], anti-inflammatory [24], antidiabetic [25], antibacterial [26], antifungal [27], anti-epileptic [28], antimalarial [29], and antileishmanial [30] and others upon suitable structural modification. The highly functionalized DHPM 10, termed MAL3-101, had been observed with effect of inducing breast cancer cell apoptosis [31]. More recently, dihydropyrimidinone have emerged as the integral backbone of several calcium channel blockers [32,33], antioxidant molecules [34], and radical scavengers [35–37]. Among the dihydropyrimidinone derivatives, compound SQ 32,547 and SQ 32,926 were developed as antihypertensive agents. [38] Initially, reduction of N-3, C-4 pi bond of the dihydropyrimidin-2(1*H*)-one was attempted with highly selective sodium cyanoborohydride [39] and other reducing agents such as borohydride and nickel boride, [40] under a variety of conditions, however, no reaction was detected and the unreacted starting dihydropyrimidin-2(1*H*)-one was recovered. It is pleasing to observe that magnesium-methanol has been implemented in a number of chemical reductions of functionalities such as α, β-unsaturated esters, [41] peroxides, [42] benzothiadiazoles, [43] aziridines, [44] α, β-conjugated nitriles, [45] ketones [46] etc. 3, 4-Dihydropyrimidin-2(1*H*)-one bear close relationship in their structure as well as cardiovascular effects with 1,4-dihydropyridines, typified by nifedipine, amlodipine and nicardipine etc. This has prompted significant attentiveness in these molecules for the past 10 years. While the 1,4-dihydropyridine are racemic, they are inherently asymmetric. However, these compounds depict identical receptor bound conformation, which has led to the binding site model and identification of conformational preferences depicting interaction with receptor sites, leading to the observed binding effects. The increasing importance of scaffold decoration of heterocycles is attested by the fact that, compared to combinatorial approach and High Throughput Screening (HTS) approach, a good number of potent drug leads have been rationally designed, identified and evaluated for various kind of biological effects. Dihydropyrimidinone **4** was synthesized by simple one-pot cyclocondensation reaction of β ketoester **1**, aldehyde **2** and urea **3** (**Scheme 1**). In the present study, a commercially viable method for the synthesis of DHPM compound was described, DFT and its biological significance had been studied.

Experimental

2. MATERIALS AND METHODS

The chemicals used in the experiments were procured from Sigma-Aldrich (India). Toluene: ethyl acetate (1:9) was used as the mobile phase in the TLC technique. Using iodine vapor, TLC spots were detected. Melting point was determined in open-end capillary and are uncorrected. Elemental analysis was conducted using a Thermo Scientific (FLASH 2000) Elemental Analyzer. FT-IR spectra was taken from a 400-4000 cm^{-1} Nicolet Avatar 330 FT-IR spectrometer using the KBr pellet technique. ^{1}H & ^{13}C-NMR was registered on a Bruker 400 MHz spectrometer using TMS as standard. Chemical changes were recorded in parts per million (ppm). ESI-Mass spectrum is measured in + ve and - ve mode on a SCIEX-API 2000 ESI-MS spectrometer (electron spray soft ionization technique) for the synthesized compound.

UV-Vis and fluorescence measurements were performed using the Perkin-Elmer LS45 fluorescence spectrophotometer with a scan rate of 1200 nm.

Synthesis of Ethyl-6-methyl-2-oxo-4-(3,4,5-trichlorophenyl)-1,2,3,4-tetrahydropyrimidine-5-carboxylate 4

The reaction mass containing ethyl acetoacetate (15 mmol), 3,4,5-trichlorobenzaldehyde (15 mmol), and urea (25 mmol) in ethanol (25 mL) in the presence of $CeCl_3.7H_2O$ (25%) were heated to reflux for 3 to 4 hours under nitrogen blanket. The reaction was monitored by TLC. Once the reaction is completed, the reaction mass temperature was brought down to about 25°C and poured onto 250 g ice (crushed) and stirred for 5–15 min. The solid was separated and suction filtered under vacuum, washed with 250 mL of water (ice-cold). The pure product was obtained by recrystallizing the wet material from hot ethanol (**Scheme 1**).
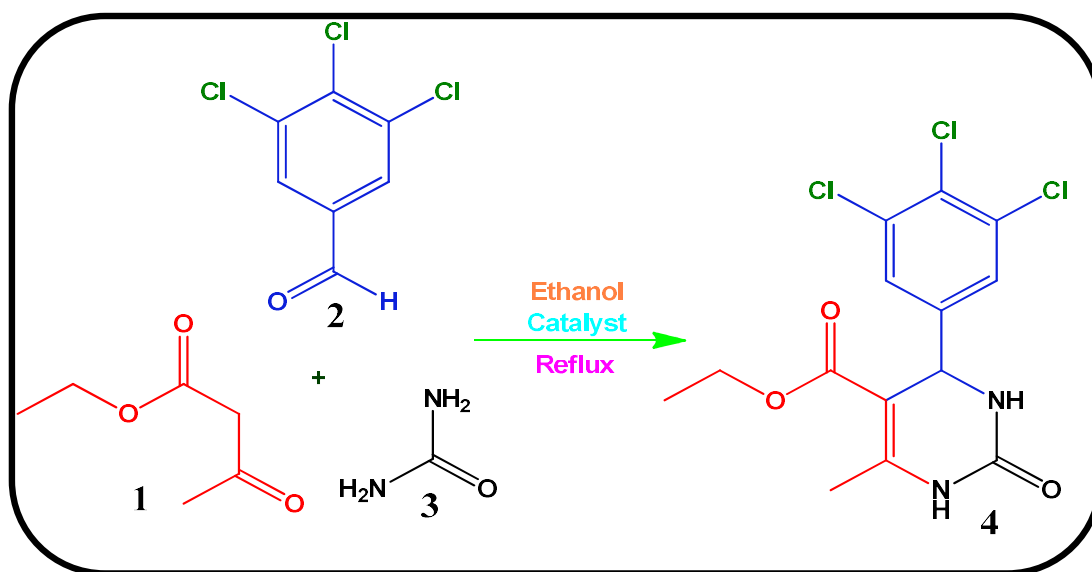
Scheme 1. Synthesis of dihydropyrimidinone **4**

Yield: 81 %; Pale yellow solid; Melting point: 222-224°C; Chemical Formula: $C_{14}H_{13}Cl_3N_2O_3$; Calculated %: C, 46.24; H, 3.60; N, 7.70; Found %: C, 46.19; H, 3.57; N, 7.69; **FT-IR (KBr) cm^{-1}**: 3214 (2° N-H stretch, amide), 2968.3 (Csp^2-H stretch, aromatics), 2937.3 (Csp^3-H stretch, alkanes), 1697 (Conjugated C=O stretch, ester), 1606.1 & 1508.4 (C=C stretch, aromatics), 1451.5 (CH_2 bend, alkanes), 1373.3 (CH_3 bend, alkanes), 1236.8, 1174.0 & 1029.4 (C-O stretch, ester), 824.3 (C-Cl stretch). **^{1}H NMR (DMSOd$_6$, 400 MHz, δppm)**: 9.17 (brs,1H, N*H*), 5.50 (brs,1H, N*H*), 7.52 (d,1H, Ar*H*), 7.51 (d,1H, Ar*H*), 5.27 (d,1H, C*H*), 4.06 (q,2H, C*H$_2$*), 2.45 (s,3H, C*H$_3$*), 1.29 (t,3H, ester-C*H$_3$*). **^{13}C NMR (DMSO-d$_6$, 400 MHz, δppm)**: 165.9, 153.6, 149.1, 142.2, 133.2, 128.5, 127.6 (2 carbon), 104.0, 60.1, 53.0, 16.0, 14.1, 13.6. ESI-MS: Calculated: m/z = 363.62; Found: m/z = 363.31 [M]$^+$ ion.

Computational details

The density functional theory calculation for the new compound **4** is done using Gaussian 03W software at B3LYP/6-31G (d,p) level. The frontier molecular atomic orbital is also analyzed on the fundamental of the HOMO-LUMO energy gap. The Mulliken atomic charges, dipole moment, polarizability, hyperpolarizability, geometrical parameters are determined.

Molecular docking Procedure

Protein preparation

Molecular docking simulation was conducted on the dihydropyrimidinone compound 4 structure and 3D structure-based pharmacophore models are used to classify the molecular interactions of alpha-mangostin and its estrogen receptor alpha (ER$_a$) derivatives (PDB ID: 2J9 M) are collected from the Brook-haven Protein Data Bank (RCSB) (http:/www.rcsb.org/pdb). Using the protein preparation wizard, the protein was pre-processed and packaged. Using a Scan and Alter panel, the unnecessary protein chains and water molecules were eliminated. In order to minimize the complex, the OPLS-2005 force field was used. The grid was generated and imported into GLIDE Docking using the generation panel of the receptor grid.

Ligand Preparation

The molecular structure of Receptor 4 was drawn using Chem Office 8.0 and stored in the SDF file format. The structure file of dihydropyrimidinone compound 4 was imported into project table Maestro and reduced using the force field of OPLS 2005 (Optimized Potential for Liquid Stimulation). To neutralize the compound charge and ionization, the EPIK programme was used.

Molecular Docking

The proteins and ligands prepared in silico were used with Glide for molecular docking. Extra Precession (XP docking) was used to classify the protein-ligand interaction.

Cell culture

The MCF-7 cell line (NCCS, Pune, India) was grown with 10 percent FBS and antibiotics (penicillin-100 μg/mL; streptomycin-50 μg/mL) supplemented with DMEM. In 95% air, 5% CO_2 incubator, cells are cultured at 37ºC.

Anticancer activity, Cell viability assay

Dihydropyrimidinone compound cytotoxicity was tested against MCF-7 cell lines using the 3-(4,5-dimethylthiazole-2-yl)-2,5-diphenyltetrazolium bromide (MTT) assay. At a density of 1.5×10^4 cells per well, the cells were seeded into a medium containing a 96-well plate and incubated in dihydropyrimidinone compound at a concentration ranging from 0.9 to 500 μM for 48 hours. For any treatment, triplicate wells were maintained, with 100 μL of MTT applied to each well. MTT was allowed to form formazan crystals by reacting with MTT and metabolically active cells, the well was incubated at 37ºC for 4 hrs. The medium with MTT was safely disposed from the wells after the analysis. Every well was applied to dissolve intracellular formazan crystals with 100 μL of DMSO, and the plates are shaken for 10 min. Absorption was read out at 350-500 nm using ELISA (enzyme-linked immunosorbent assay)

readers. Using a fluorescence microscope, the cell photos were analyzed. The proportion of survival was calculated using the formula:

$$\% \text{ survival} = [\text{live cell number (test)}/\text{live cell number (control)}] \times 100$$

DPPH radical scavenging assay

According to the Blois process, the DPPH assay was carried out. The reaction is based on the reduction of the free radical compound, 1,1-diphenyl-2-picrylhydrazyl (DPPH) which is a stable. This gives rise to a reduced form with the lack of pale violet color when DPPH reacts with a product that can donate a nitrogen atom; pale yellow color remained from the phenyl group. The compound antioxidant activity, using the DPPH process, was calculated in terms of nitration donation or radical scavenging capacity. Different sample concentrations such as 20, 40, 60, 80, 100μg / mL, and reference compounds of ascorbic acid were prepared in an ethanol solution of 0.3mM of DPPH. The mixture was violently shaken and let to stand for 30 minutes in the dark place about 25ºC. Then, at 350-500 nm against a blank, the absorbance was assessed. The inhibition percentage was calculated by comparing the absorption values of the control samples and the test samples. The percentage of inhibition was calculated using the below given formula:

$$\text{Percentage inhibition (I \%)} = (A_{control} - A_{sample} /A_{control}) \times 100$$

Where '$A_{control}$' is the control absorbance and 'A_{sample}' is the sample absorbance. The compound's antioxidant activity was expressed as IC_{50}. (IC_{50} – concentration of the compound required to achieve a 50% radical scavenging activity). Ascorbic acid was used as a positive control.

ABTS Radical Scavenging Assay

The radical scavenging behavior of ABTS was calculated by Re method-azinobis (3-ethylbenzo thiazoline-6-sulfonic acid) (ABTS) radical cation (ABTS*+) was formed by reacting at room temperature at equivalent amounts of 7 mM ABTS salt and 2.45 mM ammonium persulfate. The mixture was allowed to stand for 16 hours about 25ºC in the dark place. The samples were allowed to react at various concentrations such as 20, 40, 60, 80, 100μg/mL, with 900 μL of ABTS solution. The absorbance reading was taken after 20 minutes at 350-500 nm, and was compared with the power. The experiments were all carried out in triplicate. The proportion of ABTS+ inhibition by the sample was determined as follows:

$$\text{Percentage inhibition (I \%)} = (A \text{ control} - A \text{ sample} /A \text{ control}) \times 100$$

3. RESULTS AND DISCUSSION

Chemistry

Dihydropyrimidinone chemistry has been actively pursued recently. A number of high yielding variants of the traditional three-component Biginelli condensation employing a various reaction conditions / technique have been developed using different catalysts, reagents and solvents. Although the dihydropyrimidinone **4** can be synthesised in a one-pot Biginelli condensation (**Scheme 1**), systematically designed DHPMs have more often been obtained only through chemical functionalization of an appropriate site of the dihydropyrimidinone **4**

core. There are six possible sites (**Figure 1**) around the dihydropyrimidinone **4** ring where modification / functionalization has been achieved. In this thesis, we have carried out some useful regioselective synthetic transformations on dihydropyrimidinone **4**, which were either not known or lacked practical utility. We have also developed an approach for transformation of Biginelli dihydropyrimidinone compound **4** has also been evaluated as modulators of cytostatic activity. Also, we have addressed N-1 and N-3 diversification for gaining access to enantiomerically pure dihydropyrimidinone **4** and have presented satisfactory characteristic data of both the enantiomers, which is extremely scanty in the literature. In yet another instance, while performing N-3 acylation, we isolated N-1, N-3 diacyl dihydropyrimidinone **4**, which were found to transform to N-3 acyl derivative through deacylation at N-1. Based upon this observation, we developed a useful protocol for "acyl group transfer" to various nucleophiles and have investigated scope and limitation of this reaction.
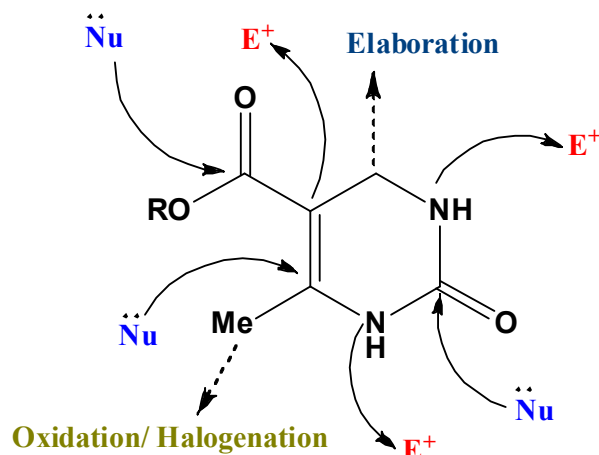

Fig 1. Possibilities of structural diversification of the dihydropyrimidinone scaffold

Experimental spectroscopic properties of compound 4

The UV Visible spectrum of compound **4** was recorded in chloroform solvent and it showed two absorption bands and the first absorption band in the range of 225 nm at a maximum absorption energy level of compound **4**. The medium absorption lays at 281nm that can be intramolecular charge transfer. The higher λ_{max} is observed for compound **4**. The absorption spectrum is shown in **Fig. 2** and **3**. These absorption variations are also mostly similar with the transition of intramolecular charge transfer between both the donor and the acceptor unit, which corresponds due to the chlorine group. This is based on the conjugation in donor-pi-acceptor arrangement in the molecule. In our study we found a tendency that the compound **4** have redshift, compound **4** displayed absorption at 242 & 280 nm and emission at 375 & 386 nm in chloroform, absorption at 242 & 280 nm and emission 370 & 400 nm in methanol. The complete photophysical properties compound **4** is presented in **Table I** and displayed in **Figs. 2** and **3** for the two different solvents, chloroform & methanol having different polarities.
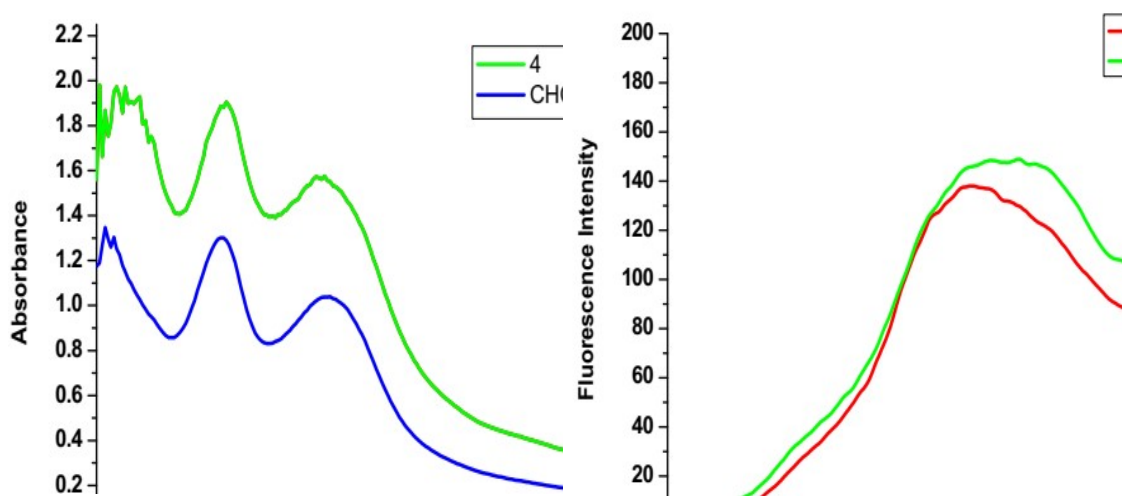
Fig. 2 (a) Absorption and (b) normalized emission spectra of compound **4** with CHCl$_3$
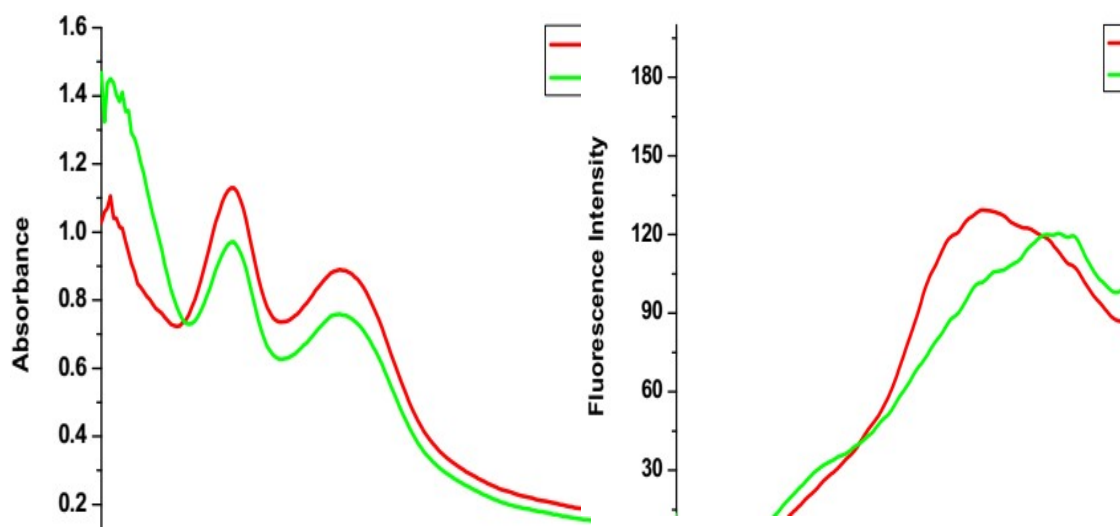

Fig. 3 (a) Absorption and (b) normalized emission spectra of compound **4** with MeOH

Table I - Absorption and emission properties of compound **1**

Compound	Solvent	λ_{max} nm	λ_{max} cm^{-1}	ε	λ_{max} nm	λ_{max} cm^{-1}	Δv cm^{-1}
1	CHCl$_3$	242&280	2.73	3.95	375&386	13188.73	7982.10
	MeOH	242&280	2.66	3.89	370&400	13179.80	7950.03

Compound 4 was a negligible difference in the absorption maxima and emission maxima has been step by step shifting towards the red side of the UV-visible spectrum with the raise in the polarity of the solvent.

Computational Analysis

Geometry optimization

All computational optimization became recorded to optimized structural parameters of compound **4**. The geometric parameters evaluated at the density functional theory the obtained optimized geometry was displayed in **Fig. 4**.
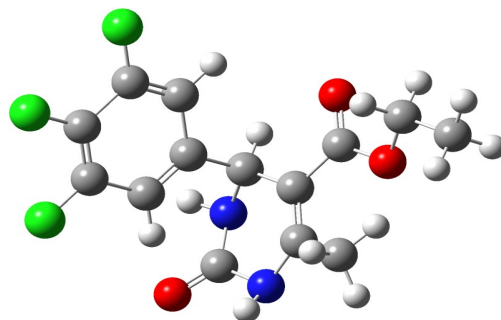

Fig. 4 Optimized structures of compound

Geometrical analysis

The structural parameters, like bond lengths, bond angles and dihedral angles of the compound **4** were determined at B3LYP level theory with 6-31G (d,p) basis set the following numbering scheme for the atom of the molecule shown in **Fig. 5**.
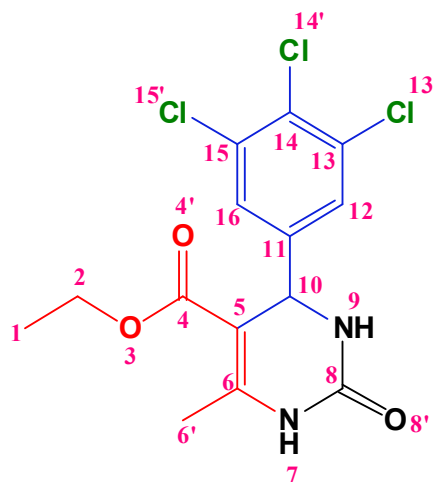

Fig. 5 - Numbering pattern of dihydropyrimidinone

NLO Studies

The first-order molecular hyperpolarizability response of compound **4** at the molecular level is demonstrated by the density functional theory (DFT) method. The beta value of compound **4** is 5.71 times more than urea. Thus, we assume that better nonlinear optical properties.

Table II - Dipole moment (μ), polarizability (α) (x10^{-24} esu) of dihydropyrimidinone **4**

Parameter	Dipole moment (Debye)
	4
μ_x	1.6900
μ_y	-2.2804
μ_z	-2.4545
μ_{total}	3.7524
Parameter	Polarizability (a.u)
α_{xx}	143.6573
α_{yy}	157.9633
α_{zz}	143.6212
α_{xy}	1.7669
α_{xz}	8.7940
α_{yz}	0.2865
α_o (esu)x10^{-23}	2.2
$\Delta\alpha$ (esu) x10^{-24}	2.75

Table III - Hyperpolarizability β_{tot} (x10^{-30} esu) values of dihydropyrimidinone **4**

Parameter	Hyperpolarizability (a.u)
	4
β_{xxx}	12.0312
β_{yyy}	-92.8360
β_{zzz}	-4.1173
β_{xyy}	16.6715
β_{xxy}	-29.9014
β_{xxz}	-29.3720
β_{xzz}	-9.8093
β_{yzz}	-11.5294
β_{yyz}	-25.7876
β_{xyz}	5.7328
β_0 (esu) x10^{-30}	8.38

Computed dipole moment (μ), polarizability (α) and hyperpolarizability (β) of the specimen are 3.75, 2.75 x 10^{-24} and 8.38 x 10^{-30} esu are given in **Table II** and **III**.

HOMO-LUMO analysis

The FMOs plays a key role in the reactivity and chemical stability of the target structure. The HOMO is a represent the electron donor, LUMO is a represent an electron acceptor. The DFT method using the basis set of level B3LYP/6-31G (d,p) to produce both the very best higher occupied molecular orbital and the lower unoccupied molecular orbits. The HOMO-LUMO energy of the compound 4.115 eV, and the HOMO-LUMO energy gap significant in the charge transfer intramolecular interaction occurs within the target structure. The HOMO-LUMO orbital pictures display in **Fig. 6.** The negative and positive phase is indicated in green and red color takes part in chemical stability and transport properties of molecular orbitals.
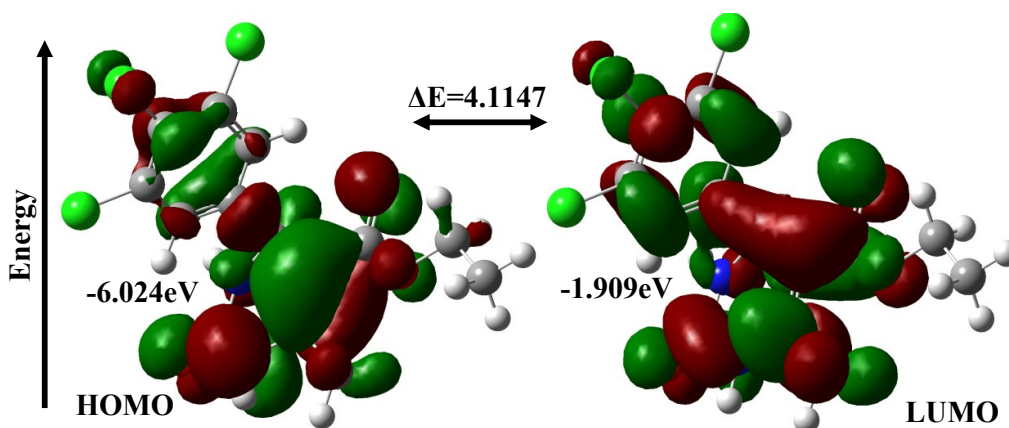
Fig. 6 HOMO and LUMO molecular orbital in gas phase of dihydropyrimidinone **4**

The energy difference of FMO is playing a considerable role in, electro negativity, chemical reactivity, electrophilicity, hardness, the softness of the suitable molecule. Differences in orbital energy from HOMO-LUMO are illustrated in **Table IV**.

Table IV - Calculated energy values (eV) of dihydropyrimidinone **4** in gas phase

B3LYP/6-311++G(d,p)	4
E_{HOMO}	-6.024
E_{LUOMO}	-1.909
$E_{LUMO\text{-}HOMO}$	4.115
Electronegativity	-3.967
Hardness	2.057
Electrophilicity index	3.825
Softness	6.613

MEP analysis

Electron density surface MEP is used for anticipating electrostatic potential surface area, physicochemical properties, and hydrogen bonding interaction particularly exhibiting atoms in molecules. The **Fig. 7** shows red color (negative) potential surface which is confined to the nitrogen atoms due the nucleophilic nature. The blue color (positive) region is confined around the hydrogen atoms the electrophilic nature.
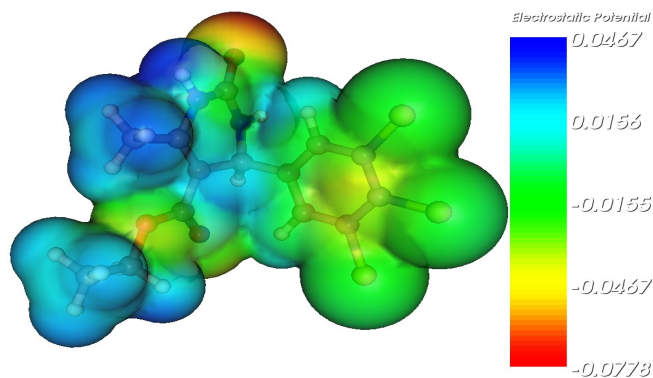

Fig. 7 MEP diagram of compound 1

Mulliken atomic charge analysis

The charge on atoms within molecule is crucial factor to decide the bonding capacity of molecule. The atomic charge in molecule provides a clear picture of the distribution of electron density over the molecule. The Mulliken atomic charge of the compound **4** in computed was shown in **Table V** and **Fig. 8**. The hydrogen atoms bound to C-4, C-6, Cl13' and Cl14' atoms have more positive charges than the other hydrogen atoms.
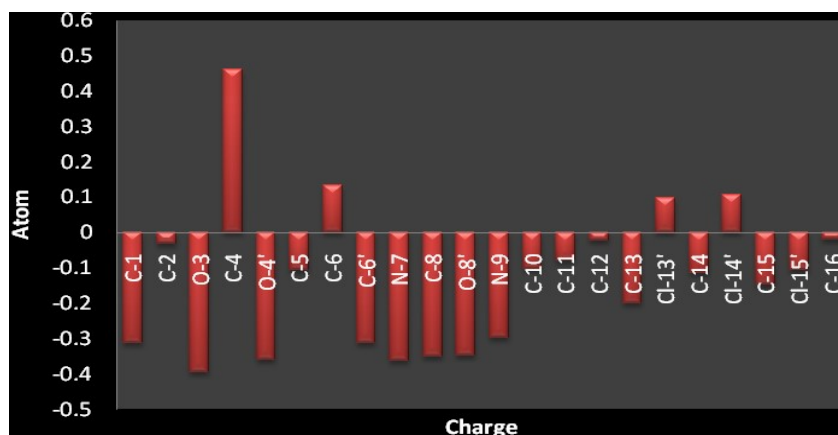

Fig. 8 Mulliken atomic charge distribution of dihydropyrimidinone **4**

Table V - Mulliken atomic charges of dihydropyrimidinone **4**

Atom	4	Atom	4
C-1	-0.313	N-9	-0.297
C-2	-0.032	C-10	-0.102
O-3	-0.396	C-11	-0.079
C-4	0.461	C-12	-0.024
O-4'	-0.361	C-13	-0.201
C-5	-0.107	Cl-13'	0.099
C-6	0.133	C-14	-0.114
C-6'	-0.314	Cl-14'	0.108
N-7	-0.362	C-15	-0.148
C-8	-0.350	Cl-15'	-0.107
O-8'	-0.348	C-16	-0.020

This end results occurred shows their binding effect to electronegative charge. It is significant to stress upon that the intermolecular H-bonds formed in the compound have corroboration these results. Among the Mulliken charge of carbon atoms of compound **4**, that of C-4 appears to be the highest value (0.461). On the other hand, C-1, O-3, O4', C-6', N-7, C-8, O-8' and N-9 atoms has the most electronegative charge values of compound **4** is (-0.313, -0.396, -0.361, -0.314, -0.362, -0.350, -0.348 and -0.297 respectively). The Mulliken charge value as anticipated for the electronegativity of these compound, the maximum atomic charge is noticed on the oxygen atom when compared with other atoms because oxygen group highly electronegative atoms.

Molecular docking analysis

The human receptor-alpha ligand-binding molecular domain structure within the potent inhibitor (PDB ID: 3ERT) was acquired from the Protein Data Bank, and the refined and molecular structure was used for analysis. We determined that the synthesized compound **4** represent significant London dispersion force of interactions in the surrounding hydrophobic residues ALA 359, GLU 353, ARG 394, LEU 391, THR 347, VAL 418, ILE 424, and form hydrogen bonds in the Helix 12 through a group of hydrazides. Of these, the compound best scoring pose **4** from the molecular docking analysis is proved in the **Fig 9**. Together with receptor residues that interact within binding sites with the ligand. From the molecular docking, we noticed that the molecule **4** showed the best glide score (-8.955 kcal/mol) respectively.

Table VI - Molecular docking studies of dihydropyrimidinone 4

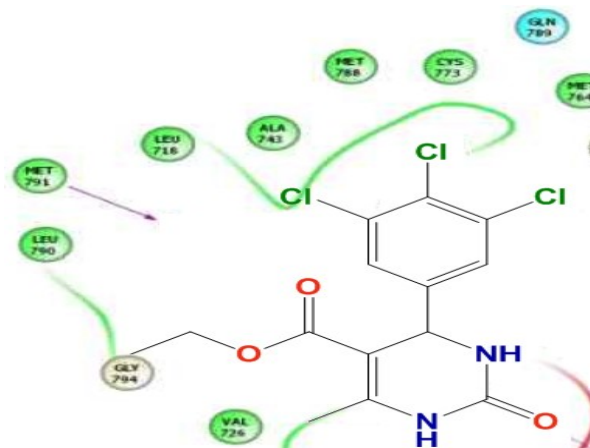| Compounds	glide gscore	glide evdw	glide ecoul	glide energy	Interacting Residues
4	-8.955	-24.971	-0.307	-25.277	GLU 353, ASP 351, ALA 350, LEU 349, THR 347, LEU 346, MET 343
Regorafenib	-9.006	-43.643	-7.074	-50.717	-
glide evdw = van der Waals interaction energies, glide ecoul = Coulomb interaction energies					

Fig. 9 Molecular docking study of PDB code: 2J9M with the various non-covalent interactions of dihydropyrimidinone **4**/2d image

The compound **4** showed a binding affinity to the receptor of estrogen (ER), and their docking scores associated with the standard (**Table 6**). The compound **4** have the highest binding energy in the -25.277 kcal/mol, respectively. The studies were well known, and the results were reported.

Cytotoxicity assay

The compound **4** were evaluated using MTT assay for anticancer activities against cell lines of breast cancer (MCF-7). The results estimated that the compound **4** were seen in cytotoxic potential in MCF-7 cell lines as opposed to standard ascorbic acid within the IC_{50} values of 10-50μg/mL. The compound **4** has demonstrated maximum activity in opposition to MCF-7 cancer cell lines. Compound **4** cytotoxicity responses are applied with varying concentrations. This is evident from the cellular imagery. Hence, this result within compound **4** is an efficient candidate for observation changes in the intracellular concentration under certain biological conditions, and it has treated with varied concentration of compound **4** for up to 5 hrs.
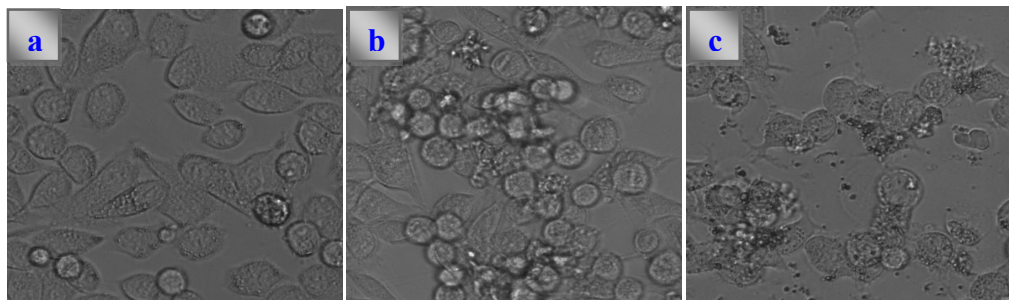

Fig. 10 Live cell image of dihydropyrimidinone **4**: (a) before and (b and c) after treatment with dihydropyrimidinone **4** examined by fluorescence microscopy.

As displayed in (**Fig 10**), 20 μM concentration of compound **4** did show crucial cytotoxic effects on MCF-7 cancer cells for at least up to 4 hrs. A cell with high concentrations of tested compound was tested for 2 days. The compound-treated MCF-7 line **4** display microscopic images of cancer control cells and apoptotic morphological variations in (**Fig 10**). Cytotoxicity is indicated as a concentration of inhibits cancer cell growth by 50% (IC_{50}). IC_{50} values of compound **4** exhibited moderate cell death in breast cancer cells (45 μM). The compound **4** exhibit strong inhibition of 50% respectively on the MCF-7 cell lines with IC_{50} values. The IC_{50} values of the compounds (**Fig. 11**) suggest that compound **4** possessed a more potent inhibitory effect against the cancer cells.
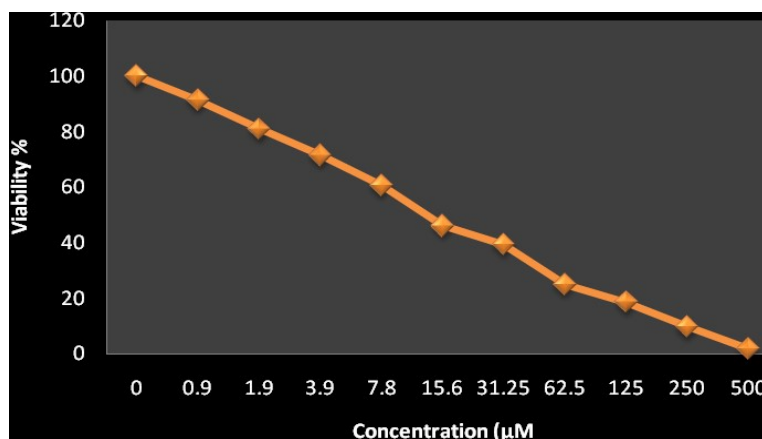

Fig. 11 The IC_{50} values of dihydropyrimidinone **4** against MCF7 cell lines.

Compound **4** having 3 Cl group and shows the highest IC_{50} value, convincing us to suggest that the electronic effect may be one of the factors in determining the anticancer activities of compound **4**. IC_{50} values of dihydropyrimidinone compound **4** in opposition to MCF-7 cell lines decisions are given in (**Table VII**).

Table VII - The IC_{50} values of dihydropyrimidinone **4** against MCF7 cell lines.

Anticancer effect of dihydropyrimidinone 4 on MCF7 cell line	
Concentration (µM)	Cell Viability %
	4
0	100
0.9	91.41±0.48
1.9	80.980.27
3.9	71.56±0.19
7.8	60.70±0.22
15.6	46.11±0.66
31.25	39.35±0.15
62.5	25.02±0.26
125	18.57±0.34
250	9.68±0.75
500	1.75±0.31

Each value is expressed as percentage of activity mean ± standard deviation (n = 3)

Antioxidant Activity

The compound was also screened for *in vitro* antioxidant evaluation by DPPH and ABTS method and their free radical scavenging property was reported.

DPPH radical scavenging assay

The synthesized compound showed interesting antioxidant activity compared to standard. Among them, compound **4** was found to be more potent with IC_{50} value of 39.59 µM respectively, comparable to standard with IC_{50} values 47.43 µM. Presence of chloro group on phenyl ring showed promising activity. Replacement of electron releasing groups on phenyl ring linked to both the moieties showed moderate activity Presence of oxygen atom at 2nd position of dihydropyrimidinone ring has improved antioxidant effect. The percentage inhibition values and IC_{50} values are tabulated in **Table VIII** and illustrated in **Fig. 12**.

Table VIII - The DPPH radical scavenging activity of the compound 4

Antioxidant **effect of compound 4**		
Concentration (µg/mL)	% Inhibition	
	4	Standard
20	28.19±0.27	22.11±0.16
40	46.23±0.61	37.09±0.23
60	64.30±0.70	52.13±0.55
80	76.58±0.36	78.64±0.27
100	107.11±0.79	94.09±0.13
IC_{50}(µM)	39.59	47.43

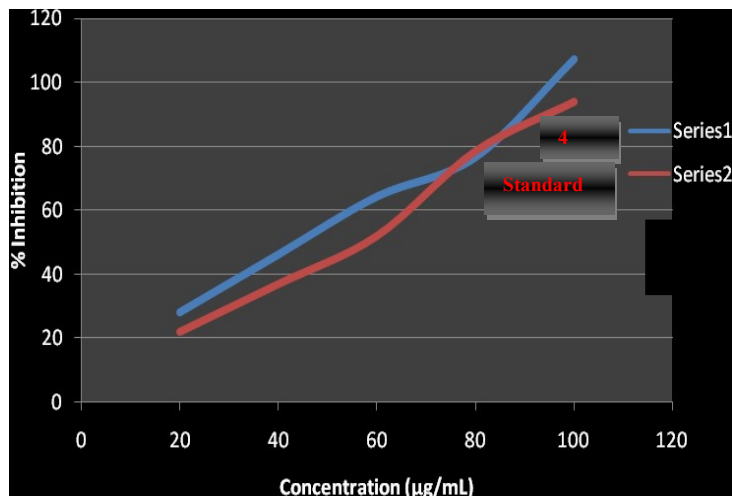Each value is expressed as percentage of activity mean ± standard deviation (n = 3)

Fig. 12 *Invitro* antioxidant activity by DPPH method of compound **4**

ABTS Radical Scavenging Assay

The results of *invitro* antioxidant activity by ABTS method shows that the screened compound **4** was found to be exhibiting moderate activity that of standard, with IC_{50} values of 32.31 µM. SAR studies of ABTS assay revealed the following results, Presence of chloro groups on the phenyl ring of both heterocyclic moieties exhibited good radical scavenging ability. Presence of oxygen atom at 2nd position of dihydropyrimidinone ring has improved antioxidant effect. The percentage inhibition values are given in **Table. IX**, and illustrated in **Fig. 13**.

Table IX - The ABTS radical scavenging activity of the compound 4

Antioxidant **effect of compound 4**		
Concentration (µg/mL)	**% Inhibition**	
	4	**Standard**
20	32.51±0.32	28.11±0.29
40	59.17±0.67	45.84±0.21
60	71.32±0.21	60.18±0.43
80	90.28±0.60	87.96±0.11
100	113.61±0.22	101.84±0.43
IC_{50}(µM)	32.31	40.62

Each value is expressed as percentage of activity mean ± standard deviation (n = 3)
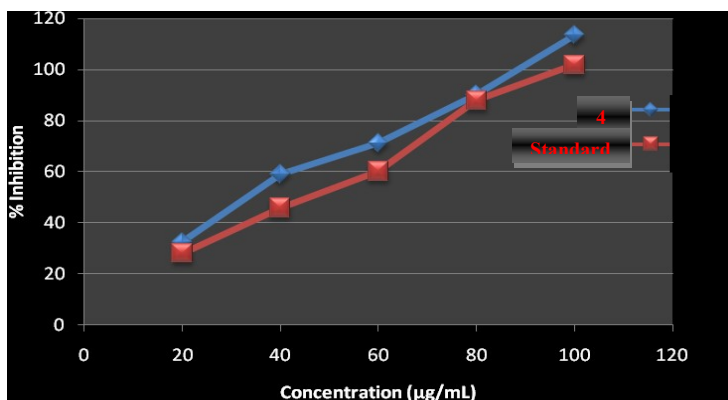
Fig. 13 *In vitro* antioxidant activity by ABTS method of compound **4**

4. CONCLUSION

It is worth mentioning that *Ethyl-6-methyl-2-oxo-4-(3,4,5-trichlorophenyl)-1,2,3,4-tetrahydropyrimidine-5-carboxylate* **4** screened for their inhibitory role and therapeutically important class of compound. The entitled work describes the Biginelli reaction for the dihydropyrimidinone synthesis. The purity of the compound was established as single spot by Thin Layer chromatography. The compound 4 structure was ascertained by FT-IR, [1]H&^{13}C NMR, LC-Mass, UV-vis and fluorescence spectral analysis. The preferred conformation was depicted for the dihydropyrimidinone 4 using DFT-B3LYP/6-31G (d,p) level of calculations. The HOMO-LUMO, Mulliken atomic charges, and molecular electrostatic potential surface are determined for dihydropyrimidinone 4. NBO analysis depicts the intramolecular charge transfer due to the stabilization of the system. Molecular docking is additionally performed in order to explain the response of the dihydropyrimidinone 4 against breast cancers. The novel dihydropyrimidinone 4 of the in-vitro anticancer exploration have indicated the anticancer efficiency of the tested compound. In general, dihydropyrimidinone 4 implicated greater anticancer activity. The compound 4 showed exceptional anticancer activity against MCF-7 cell line. The present work details on the broad spectrum of DPPH and ABTS activity in comparison with a standard. These findings encourage us to do further studies, testing on the compound 4 as a potential candidate as anticancer agent.

5. REFERENCES

[1]. Fitzmaurice, C. Global, regional, and national cancer incidence, mortality, years of life lost, years lived with disability, and disability-adjusted life-years for 32 cancer groups, 1990 to 2015: A systematic analysis for the global burden of disease study. *JAMA Oncol.* **2017**, *3*, 524–548.

[2]. Bray, F.; Ferlay, J.; Soerjomataram, I.; Siegel, R.L.; Torre, L.A.; Jemal, A. Global cancer statistics 2018: GLOBOCAN estimates of incidence and mortality worldwide for 36 cancers in 185 countries. *CA Cancer J. Clin*. **2018**, *68*, 394–424.

[3]. Vineis, P.; Wild, C.P. Global cancer patterns: Causes and prevention. *Lancet* **2014**, *383*, 549-557.

[4]. Atwal, K. S.; Swanson, B. N.; Unger, S. E.; Floyd, D. M.; Moreland, S.; Hedberg, A.; O'Reilly, B. C. *J. Med. Chem.* **1991**, *34*, 806.

[5]. Atwal, K. S.; Rovnyak, G. C.; Schwartz, J.; Moreland, S.; Hedberg, A.; Gougoutas, J. Z.; Malley, M. F.; Floyd, D. M. *J. Med. Chem.* **1990**, *33*, 1510.

[6]. Atwal, K. S.; Rovnyak, G. C.; Kimball, S. D.; Floyd, D. M.; Moreland, S.; Swanson, B. N.; Gougoutas, J. Z.; Schwartz, J.; Smillie, K. M.; Malley, M. F. *J. Med. Chem.* **1990**, *33*, 2629.

[7]. Rovnyak, G. C.; Atwal, K. S.; Hedberg, A.; Kimball, S. D.; Moreland, S.; Gougoutas, J. Z.; O'Reilly, B. C.; Schwartz, J.; Malley, M. F. *J. Med. Chem.* **1992**, *35*, 3254.

[8]. Rovnyak, G. C.; Kimball, S. D.; Beyer, B.; Cucinotta, G.; DiMarco, J. D.; Gougoutas, J. Z.; Hedberg, A.; Malley, M.; McCarthy, J. P.; Zhang, R.; Moreland, S. *J. Med. Chem.* **1995**, *38*, 119.

[9]. Zorkun, I. S.; Sarac, S.; Celebib, S.; Erolb, K. *Bioorg. Med. Chem.* **2006**, *14*, 8582.

[10]. Sehon, C. A.; Wang, G. Z.; Viet, A. Q.; Goodman, K. B.; Dowdell, S. E.; Elkins, P. A.; Semus, S. F.; Evans, C.; Jolivette, L. J.; Kirkpatrick, R. B.; Dul, E.; Khandekar, S. S.; Yi, T. Wright, L. L.; Smith, G. K.; Behm, D. J.; Bentley, R. *J. Med. Chem.* **2008**, *51*, 6631.

[11]. Chikhale, R. V. Bhole, R. P.; Khedekar, P. B.; Bhusari, K. P. *Eur. J. Med. Chem.* **2009**, *44*, 3645.

[12]. Alam, O.; Khan, S. A.; Siddiqui, N.; Ahsan, W.; Verma, S. P.; Gilani, S. J. *Eur. J. Med. Chem.* **2010**, *45*, 5113.

[13]. Singh, K.; Arora, D.; Poremsky, E.; Lowery, J.; Mreland, R. S. *Eur. J. Med. Chem.* **2009**, *44*, 1997.

[14]. Barrow, J. C.; Nantermet, P. G.; Selnick, H. G.; Glass, K. L.; Rittle, K. E.; Gilbert, K. F.; Steele, T. G.; Homnick, C. F.; Freidinger, R. M.; Ransom, R. W.; Kling, P.; Reiss, D.; Broten, T. P.; Schorn, T. W.; Chang, R. S. L.; O'Malley, S. S.; Olah, T. V.; Ellis, J. D.; Barrish, A.; Kassahun, K. ; Leppert, P.; Nagarathnam, D.; Forray, C. *J. Med. Chem.* **2000**, *43*, 2703.

[15]. Mayer, T. U.; Kapoor, T. M.; Haggarty, S. J.; King, R. W.; Schreiber, S. L.; Mitchison, T. J. *Science* **1999**, *286*, 971.

[16]. Haggarty, S. J.; Mayer, T. U.; Miyamoto, D. T.; Fathi, R.; King, R. W.; Mitchison, T. J.; Schreiber, S. L. *Chem. Biol.* **2000**, *7*, 275.

[17]. Maliga, Z.; Kapoor, T. M.; Mitchison, T. J. *Chem. Biol.* **2002**, *9*, 989.

[18]. DeBonis, S.; Simorre, J.-P.; Crevel, I.; Lebeau, L.; Skoufias, D. A.; Blangy, A.; Ebel, C.; Gans, P.; Cross, R.; Hackney, D. D.; Wade, R. H.; Kozielski, F. *Biochemistry* **2003**, *42,* 338.

[19]. Russowsky, D.; Canto, R. F. S.; Sanches, S. A. A.; D'Oca, M. G. M.; Fátima, A.; Pilli, R. A.; Kohn, L. K.; Antônio, M. A.; de Carvalho, J. E. *Bioorg. Chem.* **2006**, *34*, 173.

[20]. Deres, K.; Schroeder, C. H.; Paessens, A.; Goldmann, S.; Hacker, H. J.; Weber, O.; Kraemer, T.; Niewoehner, U.; Pleiss, U.; Stoltefuss, J.; Graef, E.; Koletzki, D.; Masantschek, R. N. A.; Reimann, A.; Jaeger, R.; Gro, R.; Beckermann, B.; Schlemmer, K.-H.; Haebich, D.; Ruebsamen-Waigmann, H. *Science* **2003**, *299*, 893.

[21]. Pagano, N.; Teriete, P.; Mattmann, M.E.; Yang, L.; Snyder, B.A.; Cai, Z.; Heli, M.L.; Cosford, N.D.P. An integrated chemical biology approach reveals the mechanism of action of HIV replication inhibitors. *Bioorg. Med. Chem.* **2017**, *25*, 6248–6265.

[22]. Zhu, X.; Zhao, G.; Zhou, X.; Xu, X.; Xia, G.; Zheng, Z.; Wang, L.; Yang, X.; Song, L. 2, 4-Diaryl-4, 6, 7, 8-tetrahydroquinazolin-5 (1H)-one derivatives as anti-HBV agents targeting at capsid assembly. *Bioorg. Med. Chem. Lett.* **2010**, *20*, 299–301.

[23]. Matias, M.; Campos, G.; Santos, A.O.; Falcão, A.; Silvestre, S.; Alves, G. Potential antitumoral 3, 4-dihydropyrimidin-2-(1 H)-ones: Synthesis, in vitro biological evaluation and QSAR studies. *RSC Adv.* **2016**, *6*, 84943–84958.

[24]. Lauro, G.; Strocchia, M.; Terracciano, S.; Bruno, I.; Fischer, K.; Pergola, C.; Werz, O.; Riccio, R.; Bifulco, G. Exploration of the dihydropyrimidine scaffold for the development of new potential anti-inflammatory agents blocking prostaglandin E2 synthase-1 enzyme (mPGES-1). *Eur. J. Med. Chem.* **2014**, *80*, 407–415.

[25]. Dhumaskar, K.L.; Meena, S.N.; Ghadi, S.C.; Tilve, S.G. Graphite catalyzed solvent free synthesis of dihydropyrimidin-2 (1H)-ones/thiones and their antidiabetic activity. Bioorg. *Med. Chem. Lett.* **2014**, *24*, 2897–2899.

[26]. Akhaja, T.N.; Raval, J.P. 1, 3-Dihydro-2H-indol-2-ones derivatives: Design, synthesis, in vitro antibacterial, antifungal and antitubercular study. *Eur. J. Med. Chem.* **2011**, *46*, 5573–5579.

[27]. Wani, M.Y.; Ahmad, A.; Kumar, S.; Sobral, A.J.F.N. Flucytosine analogues obtained through Biginelli reaction as efficient combinative antifungal agents. *Microb. Pathog.* **2017**, *105*, 57–62.

[28]. Lewis, R.W.; Mabry, J.; Polisar, J.G.; Eagen, K.P.; Ganem, B.; Hess, G.P. Dihydropyrimidinone positive modulation of delta-subunit-containing gamma-aminobutyric acid type A receptors, including an-linked mutant variant. *Biochemistry* **2010**, *49*, 4841–4851.

[29]. Bhatt, J.D.; Chudasama, C.J.; Patel, K.D. Diarylpyrazole Ligated Dihydropyrimidine Hybrids as Potent Non-Classical Antifolates and Their Efficacy Against Plasmodium falciparum. *Arch. Pharm.* **2017**, *350*, 1700088.

[30]. Rashid, U.; Sultana, R.; Shaheen, N.; Hassan, S.F.; Yaqoob, F.; Ahmad, M.J.; Iftikhar, F.; Sultana, N.; Asghar, S.; Yasinzai, M.; et al. Structure based medicinal chemistry-driven strategy to design substituted dihydropyrimidines as potential antileishmanial agents. *Eur. J. Med. Chem.* **2016**, *115*, 230–244.

[31]. Rodina, A.; Vilenchik, M.; Moulick, K.; Aguirre, J.; Kim, J.; Chiang, A.; Litz, J.; Clement, C.C.; Kang, Y.; She, Y.; et al. Selective compounds define Hsp90 as a major inhibitor of apoptosis in small-cell lung cancer. *Nat. Chem. Biol.* **2007**, *3*, 498.

[32]. Teleb, M.; Zhang, F.X.; Farghaly, A.M.; Wafa, O.M.A.; Fronczek, F.R.; Zamponi, G.W.; Fahmy, H. Synthesis of new N3-substituted dihydropyrimidine derivatives as L-/T-type calcium channel blockers. *Eur. J. Med. Chem.* **2017**, *134*, 52–61.

[33]. Putatunda, S.; Chakraborty, S.; Ghosh, S.; Nandi, P.; Chakraborty, S.; Sen, P.C.; Chakraborty, A. Regioselective N1-alkylation of 3, 4-dihydropyrimidine-2 (1H)-ones: Screening of their biological activities against Ca2+-ATPase. *Eur. J. Med. Chem.* **2012**, *54*, 223–231.

[34]. Gangwar, N.; Kasana, V.K. 3, 4-Dihydropyrimidin-2 (1H)-one derivatives: Organocatalysed microwave assisted synthesis and evaluation of their antioxidant activity. *Med. Chem. Res.* **2012**, *21*, 4506–4511.

[35]. Kumar, B.R.P.; Sankar, G.; Baig, R.B.N.; Chandrashekaran, S. Novel Biginelli dihydropyrimidines with potential anticancer activity: A parallel synthesis and CoMSIA study. *Eur. J. Med. Chem.* **2009**, *44*, 4192–4198.

[36]. de Vasconcelos, A.; Oliveira, P.S.; Ritter, M.; Freitag, R.A.; Romano, R.L.; Quina, F.H.; Pizzuti, L.; Pereira, C.M.P.; Francieli, M.; Stefanello, F.M.; Alethéa, G.; Barschak, A.G. Antioxidant capacity and environmentally friendly synthesis of dihydropyrimidin-(2H)-ones promoted by naturally occurring organic acids. *J. Biochem. Mol. Toxicol.* **2012**, *26*, 155–161.

[37]. Stefani, H.A.; Oliveira, C.B.; Almeida, R.B.; Pereira, C.M.P.; Braga, R.C.; Cella, R.; Borges, V.C.; Savegnago, L.; Nogueira, C.W. Dihydropyrimidin-(2H)-ones obtained by ultrasound irradiation: A new class of potential antioxidant agents. *Eur. J. Med. Chem.* **2006**, *41*, 513–518.

[38]. Grover, G. J.; Dzwonczyk, S.; McMullen, D. M.; Normandin, D. E.; Parham, C. S.; Sleph, P. G.; Moreland, S. *J. Cardiovasc. Pharm.* **1995**, *26*, 289.

[39]. Lane, C. F. *Synthesis* **1975**, 135-146.

[40]. Khurana, J. M.; Kukreja, G.; Bansal, G. *J. Chem. Soc., Perkin Trans. I* **2002**, 2520-2524.

[41]. Pak, C. S.; Lee, E.; Lee, G. H. *J. Org. Chem.* **1993**, 58, 1523-1530.

[42]. Dai, P.; Dussault, P. H.; Trullinger, T. K. *J. Org. Chem.* **2004**, 69, 2851-2852.

[43]. Prashad, M.; Liu, Y.; Repic, O. *Tetrahedron Lett.* **2001**, 42, 2277-2279.

[44]. Pak, C. S.; Kim, T. H.; Ha, S. J. *J. Org. Chem.* **1998**, 63, 10006-100010.

[45]. Profitt, J. A.; Watt, D. S. *J. Org. Chem.* **1975**, 40, 127-128.

[46]. Kim, J. U.; Kim, H. D.; Seo, M. J.; Kim, H. R.; No, Z.; Ha, D.-C.; Lee, G. H. *Tetrahedron Lett*. **2006**, 47, 9-12.